

An Ankle-Foot Orthosis Powered by Artificial Pneumatic Muscles

Daniel P. Ferris^{1,2}, Joseph M. Czerniecki^{3,5}, and Blake Hannaford⁴
^{1,2}University of Michigan; ^{3,4}University of Washington
⁵VA Puget Sound Healthcare System

We developed a pneumatically powered orthosis for the human ankle joint. The orthosis consisted of a carbon fiber shell, hinge joint, and two artificial pneumatic muscles. One artificial pneumatic muscle provided plantar flexion torque and the second one provided dorsiflexion torque. Computer software adjusted air pressure in each artificial muscle independently so that artificial muscle force was proportional to rectified low-pass-filtered electromyography (EMG) amplitude (i.e., proportional myoelectric control). Tibialis anterior EMG activated the artificial dorsiflexor and soleus EMG activated the artificial plantar flexor. We collected joint kinematic and artificial muscle force data as one healthy participant walked on a treadmill with the orthosis. Peak plantar flexor torque provided by the orthosis was 70 Nm, and peak dorsiflexor torque provided by the orthosis was 38 Nm. The orthosis could be useful for basic science studies on human locomotion or possibly for gait rehabilitation after neurological injury.

Key Words: locomotion, exoskeleton, gait, rehabilitation, proportional myoelectric control

Our goal was to develop a lightweight powered orthosis for the human lower limb that could comfortably provide plantar flexion and dorsiflexion torque during walking. We intended the powered orthosis to be used for basic locomotion studies in a laboratory or for gait rehabilitation in a clinic. There are several methods for studying motor adaptation during walking in animals (Pearson, 2000), but the invasive and/or permanent nature of most methods makes them impractical for studying motor adaptation during walking in humans. In addition, a powered ankle-foot orthosis could be useful in studying the relationship between mechanical work and metabolic cost during human locomotion (Williams, 1985) because

Departments of ¹Movement Science and ²Biomedical Engineering, University of Michigan, Ann Arbor, MI 48109-2214; Departments of ³Rehabilitation Medicine and ⁴Electrical Engineering, University of Washington, Seattle, WA 98105; ⁵VA Puget Sound Healthcare System, 1660 South Columbian Way, Seattle, WA 98108.

direct measurements could be made of external power added by the orthosis. A number of robotic orthoses are being tested around the world for gait rehabilitation (Hesse, Schmidt, Werner, & Bardeleben, 2003), but none currently provide powered plantar flexion. We did not intend this orthosis to be a portable device for healthy or for neurologically impaired individuals. As a result, a self-contained computer controller and energy supply were not necessary.

Methods

We constructed the orthosis frame from carbon fiber (Figure 1) after taking a custom fit plaster cast of the participant's lower limb. Plastic joints connected the upper shank portion of the ankle-foot orthosis with the lower foot section. Titanium fittings were laminated directly into the shell between layers of carbon fiber weave. Steel ball joint rod ends (McMaster-Carr, Los Angeles) screwed into the fittings.

We used pneumatic artificial muscles to provide powered torque to the orthosis. Recent studies have quantified the force-length, force-velocity, force-activation, and bandwidth properties of artificial pneumatic muscles in detail (Davis, Tsagarakis, Canderle, & Caldwell, 2003; Klute, Czerniecki, & Hannaford, 2002; Klute & Hannaford, 2000; Klute & Hannaford, 2000; Reynolds, Repperger, Phillips, & Bandry, 2003). We constructed the artificial pneumatic muscles using latex tubing for the inner bladder, braided polyester sleeving for the muscle shell, plastic pneumatic fittings for the endcaps and nozzles, and double ear hose clamps to seal the ends (McMaster-Carr, Los Angeles). We cut the sleeving and folded it back on itself before sealing the hose clamp in order to provide an attachment loop. Steel wire transmitted force from the sleeving loops to the rod ends.

Dorsiflexor moment arm varied from 14 to 16 cm and plantar flexor moment arm was 10 cm for the range of motion during walking. A tension load sensor

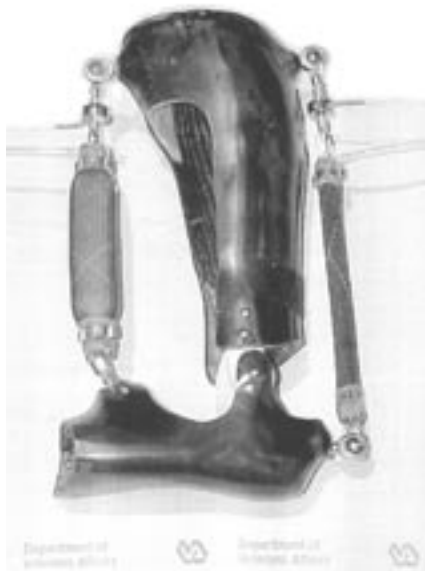


Figure 1 — Powered ankle-foot orthosis. The carbon fiber shell has an artificial pneumatic dorsiflexor (maximally inflated) and artificial pneumatic plantar flexor (relaxed) attached via titanium fittings.

(Omega Engineering, Stamford, CT) was between the muscle and the rod end to measure the force in the muscle. Clear nylon tubing supplied compressed air to the muscles (0–70 psi) from a proportional pressure regulator (Festo Corp., Hauppauge, NY). The ankle-foot orthosis had a total mass, including artificial muscles and force transducers, of 1.6 kg for a 100-kg participant.

We implemented proportional myoelectrical control through a desktop personal computer and a real-time control board (dSPACE, Northville, MI). Proportional myoelectric control uses the body's own muscle activation signals to control external devices (Hogan, 1976; Parker & Scott, 1986; Sears & Shaperman, 1991). The program regulated air pressure in the artificial pneumatic muscles proportional to the processed electromyography (EMG) signal in real time. EMG signals from the soleus and tibialis anterior were first high-pass filtered with a second-order Butterworth filter ($f_c = 20$ Hz) to remove movement artifact. Then the signals were full-wave rectified and low-pass filtered with a second-order Butterworth filter ($f_c = 10$ Hz) to smooth the signal. After passing through a threshold cutoff to eliminate background noise and an adjustable gain to scale the signal, the software sent a 0- to 10-V analog signal to the proportional pressure regulator. The relationship between EMG amplitude and artificial pneumatic muscle force was nonlinear due to force-length properties and activation dynamics of the pneumatic muscles.

We measured the activation dynamics of the artificial muscles in isometric conditions on a bench top fixture. Using a function generator, we sent a single 5-ms square pulse into the analog-to-digital board of the computer to activate the artificial pneumatic muscle. The control software converted the pulse into a control signal as described previously, and we recorded tension in the artificial pneumatic muscle. We used a zero threshold and the smallest gain that produced a clear twitch in artificial pneumatic muscle force. We also used soleus EMG to activate the artificial muscles on the bench top to calculate electromechanical delay with proportional myoelectric control (i.e., time from onset of soleus EMG burst to the increase in artificial pneumatic muscle force).

One healthy participant (age 31 years, body mass 100 kg) walked with the orthosis to test its performance during gait. The local institutional review board for protection of human subjects approved the protocol and the participant gave informed written consent. We collected 3-D joint kinematics (6 camera system at 60 Hz, Peak Motus, Peak Performance Technologies, Centennial, CO) and lower limb electromyography from the soleus and tibialis anterior (1200 Hz, Telemyo, Noraxon USA, Scottsdale, AZ) as the participant walked on a treadmill at 1.2 m/s. We used a modified Helen Hayes marker set and placed markers on the outside of the orthosis (Meinders, Gitter, & Czerniecki, 1998). The participant had practiced walking with the orthosis on three previous occasions in order to test it as it was being developed (approx. 60 minutes of previous walking experience).

For the proportional myoelectric control, we set the threshold to 25 μ V. We adjusted the gain to produce a control signal that would have a brief maximum of 10 volts based on the EMG pattern demonstrated while walking with the passive orthosis. We chose this gain to provide the greatest orthosis torque possible while still maintaining a proportional relationship. To calculate joint angle displacement, we smoothed marker position data with a fourth-order Butterworth low-pass filter ($f_c = 6$ Hz) with zero lag (KinCalc, Peak Performance Technologies). Bandwidth of the EMG amplifier was 20–500 Hz. After data collection, we processed the raw EMG signals with a second-order Butterworth high-pass filter ($f_c = 20$ Hz) with zero

time lag and full wave rectification, and then averaged together five consecutive stride cycles. We determined time of heel strike from heel marker vertical position data. A tether consisting of the plastic compressed air supply line and a cable for transmitting the muscle force signal was connected to the participant's waist.

The participant walked under four test conditions. We first collected data without the orthosis and then with the orthosis passive (6 minutes of continuous walking each time). For the third condition, soleus EMG controlled the artificial plantar flexor and the artificial dorsiflexor was not attached to the orthosis (30 minutes of continuous walking). After the third condition, the participant walked with the orthosis passive again (15 min of continuous walking). For the fourth condition, tibialis anterior EMG controlled the artificial dorsiflexor and the artificial plantar flexor was not attached to the orthosis (30 min of continuous walking). After the fourth condition, the participant again walked on the treadmill while wearing the orthosis passive (15 min of continuous walking).

Results

For the artificial pneumatic muscle twitch tests, we calculated a time to peak tension of 72 ± 5 ms and a half relaxation time of 81 ± 7 ms (mean \pm SD). The artificial pneumatic muscles had an electromechanical delay of 47 ± 7 ms between EMG burst onset and initial rise in artificial muscle tension.

The ankle-foot orthosis was comfortable to wear and did not interfere with walking when worn passively. Muscle activation patterns were very similar between walking with no orthosis and walking with the passive orthosis (Figure 2). There was slightly less ankle dorsiflexion during the beginning of the swing phase, but most joint kinematic profiles were remarkably similar for no orthosis and passive orthosis conditions. It appeared that the participant had easily accommodated to its added mass within 6 minutes of walking on the treadmill.

When the artificial plantar flexor powered the orthosis, it provided a large plantar flexor torque during stance (Figure 3). Peak torque provided by the orthosis was 70 Nm for the first minute of powered plantar flexion (Figure 3A). Peak dorsiflexion angle during stance was slightly less and occurred earlier in the stride cycle for the first minute of walking with powered plantar flexion, compared to walking with the passive orthosis (7 degrees and 47% vs. 15 deg and 53%, respectively). After 30 minutes of walking with powered plantar flexion (Figure 3B), peak plantar flexor torque, peak dorsiflexion angle, and peak dorsiflexion timing (66 Nm, 8 deg, and 48%, respectively) were similar to the first minute of powered plantar flexion.

Soleus muscle activation amplitude during the 30 minutes of powered plantarflexion averaged 53% of the amplitude during passive orthosis walking. Tibialis anterior activation amplitude during powered plantar flexion averaged 10% higher than the passive orthosis condition. After turning off the orthosis at the end of 30 minutes, muscle activation amplitudes and joint kinematic profiles quickly returned to the passive orthosis baseline values collected prior to powered plantarflexion.

When the artificial dorsiflexor powered the orthosis, the added dorsiflexor torque decreased the plantar flexion during early stance and throughout the swing phase (Figure 4). For the first minute of powered dorsiflexion (Figure 4A), peak torque provided by the orthosis was 38 Nm during early stance and 8 Nm during the stance to swing transition. As a result, peak plantar flexion during the first minute of powered dorsiflexion was 9 deg less during early stance and 12 deg less during

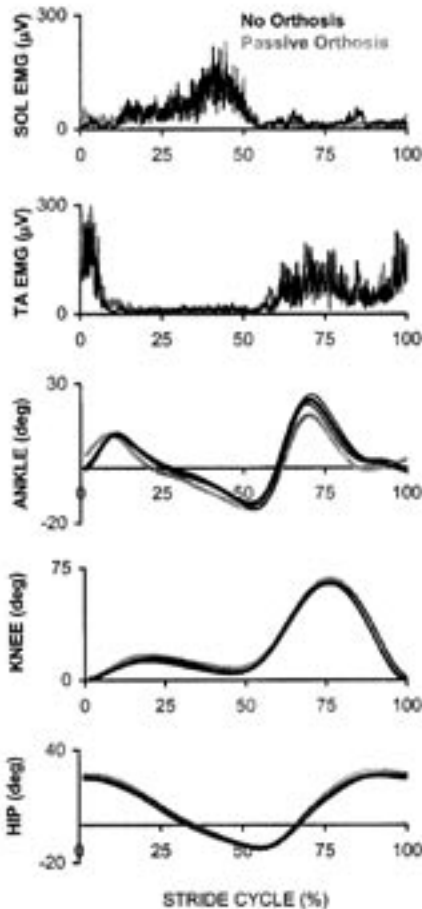


Figure 2 — Comparison of muscle activation patterns and joint kinematics for no-orthosis (black lines) and passive orthosis (grey lines) conditions. EMG graphs include mean profiles of both conditions. Joint angle graphs include mean profiles of the no-orthosis condition ($\pm 1 SD$) and of the passive orthosis standing posture. Zero degrees represents standing posture. Flexion is positive for knee and hip joint graphs. Plantar flexion is positive for ankle joint graph.

the swing phase compared to the passive condition. After 30 minutes of walking (Figure 4B), peak dorsiflexion torques (38 Nm during early stance and 6 Nm during the stance to swing transition) were similar to the first minute of powered dorsiflexion. However, peak plantar flexion after 30 minutes of walking was only 7 deg less than the passive orthosis condition during early stance, and only 6 deg less than the passive orthosis condition during swing.

Tibialis anterior muscle activation during 30 minutes of powered dorsiflexion averaged 80% of the passive orthosis condition. Soleus muscle activation amplitude was 82% of the passive orthosis condition during the first minute of powered dorsiflexion, but steadily increased during the 30 minutes of walking. By the end of the powered dorsiflexion, soleus EMG was 110% of the passive orthosis condition. Similar to the powered plantar flexion tests, muscle activation amplitudes and joint kinematic profiles quickly returned to baseline after the orthosis was turned off.

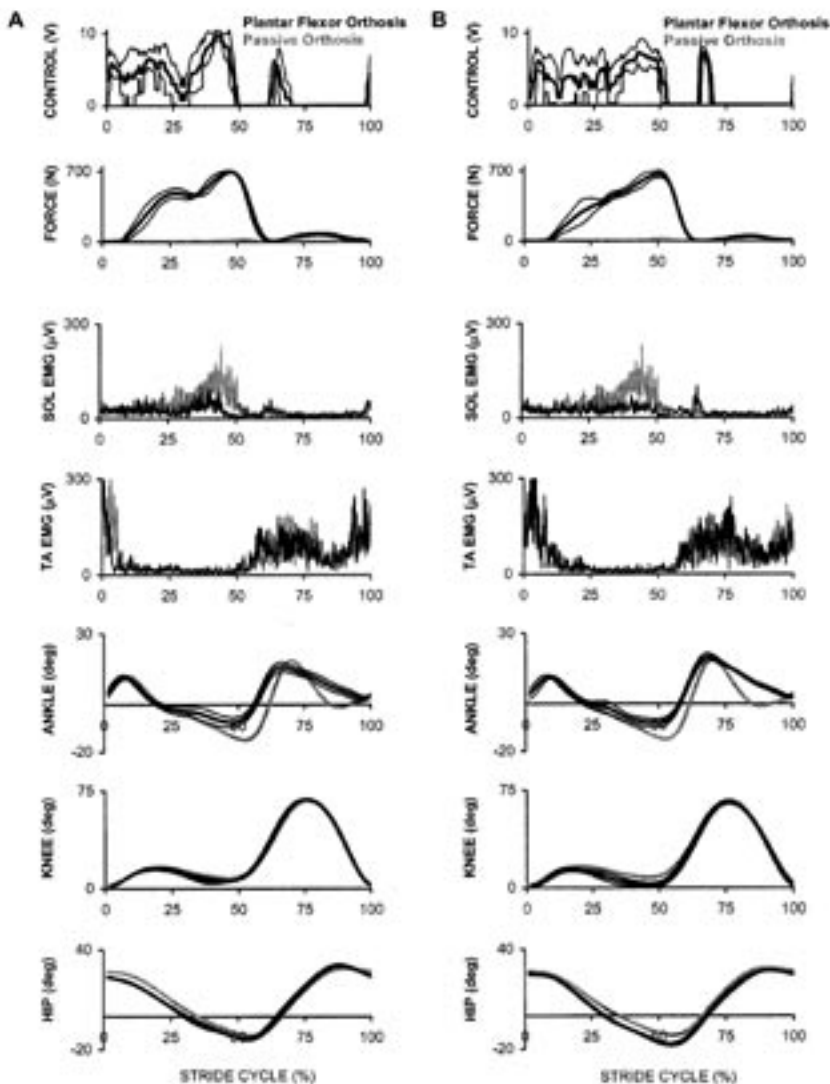


Figure 3 — Comparison of muscle activation patterns and joint kinematics for passive orthosis and powered plantar flexor orthosis conditions. Powered condition in A is after 1 minute of wearing the orthosis; powered condition in B is after 30 min of wearing the orthosis (both black lines). Passive condition in both A and B is after 6 min of wearing the orthosis (grey lines). EMG graphs include mean profiles of both conditions. Control signal, artificial muscle force, and joint angle graphs include mean profiles of powered orthosis condition (± 1 SD) and of passive orthosis condition. Zero degrees represents standing posture. Flexion is positive for knee and hip joint graphs. Plantarflexion is positive for ankle joint graph.

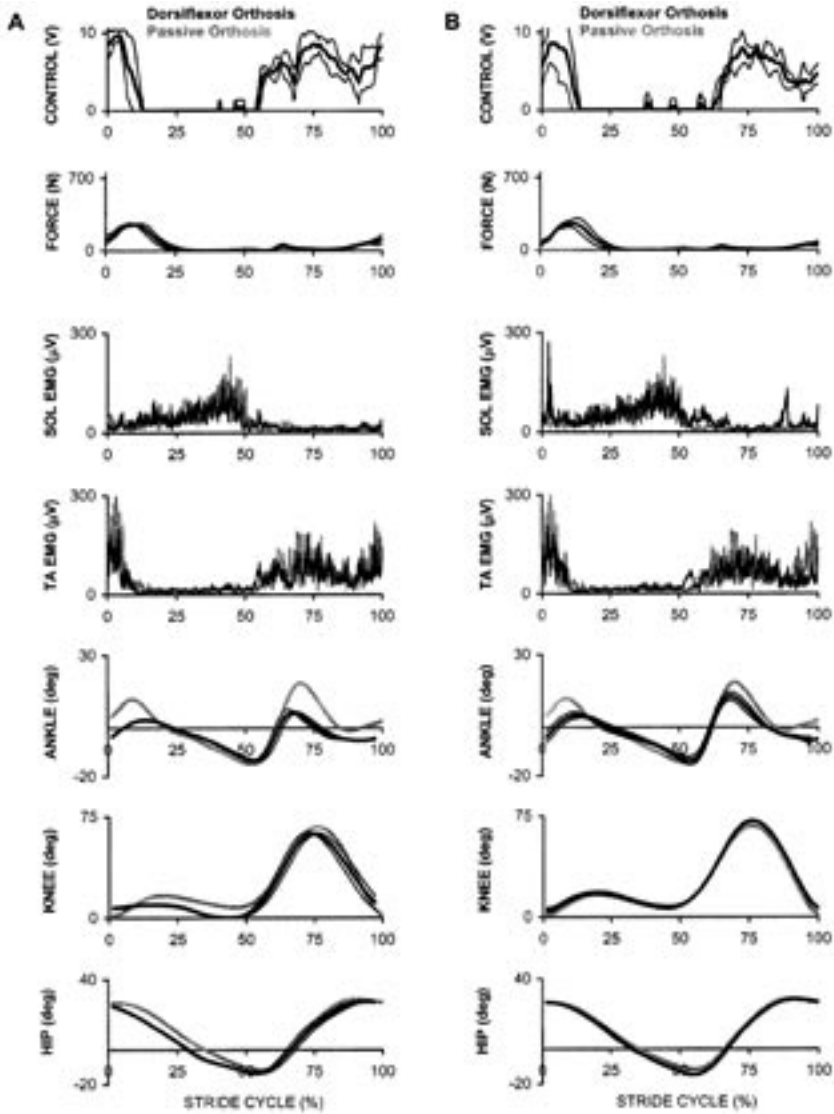


Figure 4 — Comparison of muscle activation patterns and joint kinematics for passive orthosis and powered dorsiflexor orthosis conditions. Powered condition in A is after 1 minute of wearing the orthosis; powered condition in B is after 30 min of wearing the orthosis (both black lines). Passive condition in both A and B is after 6 min of wearing the orthosis (grey lines). EMG graphs include mean profiles of both conditions. Control signal, artificial muscle force, and joint angle graphs include mean profiles of powered orthosis condition (± 1 SD) and of passive orthosis condition. Zero degrees represents standing posture. Flexion is positive for knee and hip joint graphs. Plantar flexion is positive for ankle joint graph.

Discussion

This study demonstrated that it is feasible to construct a lightweight powered orthosis providing substantial external torque to the ankle joint during human walking. Based on normative data from the literature (Sadeghi, Sadeghi, Prince, et al., 2001) and the participant's body mass, the powered orthosis was able to provide about 50% of the peak plantar flexor net muscle moment and about 400% of the peak dorsiflexor net muscle moment during unassisted walking. The magnitude of the dorsiflexor moment provided by the orthosis could easily be scaled down with the adjustable gain.

The results demonstrated a clear reduction in soleus EMG amplitude while walking with assistive plantar flexion torque (Figure 3), but it is not possible to draw conclusions about joint torque produced by the soleus. It has been well established that many factors influence the relationship between surface electromyography amplitude and biological muscle force (De Luca, 1997). Muscle length, muscle contraction velocity, superposition of motor unit action potentials, motor unit firing rate, motor unit size, and fatigue are just a few of the parameters that alter the EMG-force relationship. It would be necessary to directly measure Achilles' tendon force (Finni, Komi, & Lukkariniemi, 1998) to determine how the nervous system adjusted biological plantar flexor torque in response to the additional artificial plantar flexor torque.

There are two powered ankle-foot orthoses previously described in the literature. Blaya and Herr (2004) recently tested a polypropylene ankle-foot orthosis powered by a series elastic actuator (mass 2.6 kg). They demonstrated that an adaptive impedance controller has good potential for aiding patients with drop-foot. They did not directly state the amount of torque provided by the orthosis, but the impedance and range of motion values given suggest it was on the magnitude of 10 Nm at maximum. The other powered orthosis was constructed by Andersen and Sinkjaer (1995, 2003). Metal wires transferred mechanical power from an electromechanical motor to the orthosis (mass 0.9 kg).

Andersen and Sinkjaer used the orthosis to provide brief position perturbations to the ankle joint as a means to examine stretch reflex contributions to muscle activation. Their orthosis provided up to 45 Nm of dorsiflexor torque to the ankle, but it was not shown to be able to provide plantar flexor torque during human walking. Data presented by Andersen and Sinkjaer suggest that their orthosis has similar force bandwidth characteristics as our orthosis, but there is likely an important difference in compliance. The wire and motor orthosis has considerable impedance, limiting its backdrivability (Reinkensmeyer, Emken, & Cramer, 2004). This was a positive aspect of their orthosis given the focus of their research on reflex responses. The low compliance and high backdrivability of the artificial pneumatic muscles used in the current orthosis are much better suited for mimicking natural gait movements (Klute et al., 2002; Klute & Hannaford, 2000).

References

- Andersen, J.B., & Sinkjaer, T. (1995). An actuator system for investigating electrophysiological and biomechanical features around the human ankle joint during gait. *IEEE Transactions on Rehabilitation Engineering*, *3*, 299-306.
- Andersen, J.B., & Sinkjaer, T. (2003). Mobile ankle and knee perturbator. *IEEE Transactions on Bio-medical Engineering*, *50*, 1208-1211.

- Blaya, J.A., & Herr, H. (2004). Adaptive control of a variable-impedance ankle-foot orthosis to assist drop-foot gait. *IEEE Transactions on Neural Systems and Rehabilitation Engineering*, **12**, 24-31.
- Davis, S., Tsagarakis, N., Canderle, J., & Caldwell, D.G. (2003). Enhanced modelling and performance in braided pneumatic muscle actuators. *International Journal of Robotics Research*, **22**, 213-227.
- De Luca, C.J. (1997). The use of surface electromyography in biomechanics. *Journal of Applied Biomechanics*, **13**, 135-163.
- Finni, T., Komi, P.V., & Lukkariniemi, J. (1998). Achilles tendon loading during walking: Application of a novel optic fiber technique. *European Journal of Applied Physiology*, **77**, 289-291.
- Hesse, S., Schmidt, H., Werner, C., & Bardeleben, A. (2003). Upper and lower extremity robotic devices for rehabilitation and for studying motor control. *Current Opinion in Neurology*, **16**, 705-710.
- Hogan, N. (1976). A review of the methods of processing EMG for use as a proportional control signal. *Biomedical Engineering*, **11**, 81-86.
- Klute, G.K., Czerniecki, J.M., & Hannaford, B. (2002). Artificial muscles: Actuators for biorobotic systems. *International Journal of Robotics Research*, **21**, 295-309.
- Klute, G.K., & Hannaford, B. (2000). Accounting for elastic energy storage in McKibben artificial muscle actuators. *Journal of Dynamic Systems, Measurement and Control*, **122**, 386-388.
- Meinders, M., Gitter, A., & Czerniecki, J.M. (1998). The role of ankle plantar flexor muscle work during walking. *Scandinavian Journal of Rehabilitation Medicine*, **30**, 39-46.
- Parker, P.A., & Scott, R.N. (1986). Myoelectric control of prostheses. *Critical Reviews in Biomedical Engineering*, **13**, 283-310.
- Pearson, K.G. (2000). Neural adaptation in the generation of rhythmic behavior. *Annual Review of Physiology*, **62**, 723-753.
- Reinkensmeyer, D.J., Emken, J.L., & Cramer, S.C. (2004). Robotics, motor learning, and neurologic recovery. *Annual Review of Biomedical Engineering*, **6**, 497-525.
- Reynolds, D.B., Repperger, D.W., Phillips, C.A., & Bandry, G. (2003). Modeling the dynamic characteristics of pneumatic muscle. *Annals of Biomedical Engineering*, **31**, 310-317.
- Sadeghi, H., Sadeghi, S., Prince, F., Allard, P., Labelle, H., & Vaughan, C.L. (2001). Functional roles of ankle and hip sagittal muscle moments in able-bodied gait. *Clinical Biomechanics*, **16**, 688-695.
- Sears, H.H., & Shaperman, J. (1991). Proportional myoelectric hand control: An evaluation. *American Journal of Physical Medicine and Rehabilitation*, **70**, 20-28.
- Williams, K.R. (1985). The relationship between mechanical and physiological energy estimates. *Medicine and Science in Sports and Exercise*, **17**, 317-325.

Acknowledgments

This research was supported by NIH AR08602, NIH NS045486, and U.S. Dept. of Veterans Affairs Center Grant #A0806C. The authors greatly appreciated the help of Kristen Jaax, Glenn Klute, Jocelyn Berge, and Eric Rohr. We would especially like to thank Martin McDowell, C.P.O., for fabricating the carbon fiber shell.